OXFORD

SOT | Society of Toxicology
www.toxsci.oxfordjournals.org

TOXICOLOGICAL SCIENCES, 152(1), 2016, 40–52

doi: 10.1093/toxsci/kfw065
Advance Access Publication Date: April 12, 2016
Research Article

Generation of a New Model Rat: *Nrf2* Knockout Rats Are Sensitive to Aflatoxin B_1 Toxicity

Keiko Taguchi,* Misaki Takaku,* Patricia A. Egner,† Masanobu Morita,* Takehito Kaneko,‡ Tomoji Mashimo,‡ Thomas W. Kensler,†,§ and Masayuki Yamamoto*,[1]

*Department of Medical Biochemistry, Tohoku University Graduate School of Medicine, Aoba, Sendai 980-8575, Japan; †Bloomberg School of Public Health, The Johns Hopkins University, Baltimore, Maryland 21205; ‡Institute of Laboratory Animals, Graduate School of Medicine, Kyoto University, Kyoto 606-8501, Japan; and §Department of Pharmacology and Chemical Biology, University of Pittsburgh, Pittsburgh, Pennsylvania 15261

[1]To whom correspondence should be addressed. Fax: +81-22-717-8090. E-mail: masiyamamoto@med.tohoku.ac.jp.

ABSTRACT

The transcription factor Nrf2 (NF-E2-related-factor 2) regulates a battery of antioxidative stress-response genes and detoxication genes, and *Nrf2* knockout lines of mice have been contributing critically to the clarification of roles that Nrf2 plays for cell protection. However, there are apparent limitations in use of the mouse models. For instance, rats exhibit more suitable features for toxicological or physiological examinations than mice. In this study, we generated 2 lines of *Nrf2* knockout rats by using a genome editing technology; 1 line harbors a 7-bp deletion (Δ7) and the other line harbors a 1-bp insertion (+1) in the *Nrf2* gene. In the livers of rats homozygously deleting the *Nrf2* gene, an activator of Nrf2 signaling, CDDO-Im, could not induce expression of representative Nrf2 target genes. To examine altered toxicological response, we treated the *Nrf2* knockout rats with aflatoxin B_1 (AFB_1), a carcinogenic mycotoxin that elicits gene mutations through binding of its metabolites to DNA and for which the rat has been proposed as a reasonable surrogate for human toxicity. Indeed, in the *Nrf2* knockout rat livers the enzymes of the AFB_1 detoxication pathway were significantly downregulated. Single dose administration of AFB_1 increased hepatotoxicity and binding of AFB_1-N^7-guanine to hepatic DNA in *Nrf2* knockout rats compared with wild-type. *Nrf2* knockout rats repeatedly treated with AFB_1 were prone to lethality and CDDO-Im was no longer protective. These results demonstrate that *Nrf2* knockout rats are quite sensitive to AFB_1 toxicities and this rat genotype emerges as a new model animal in toxicology.

Key words: Nrf2; knockout rat; aflatoxin; hepatotoxicity.

INTRODUCTION

Nrf2 (NF-E2-related-factor 2) is a transcription factor and regulates genes responsible for xenobiotic detoxication, drug transport, and metabolism (Hirotsu *et al.*, 2012). Keap1 (Kelch-like-ECH-associated-protein 1) controls this activity of Nrf2. Keap1 is a Cullin 3-based ubiquitin E3 ligase, residing in the cytoplasm (Kobayashi *et al.*, 2004). Keap1 binds and ubiquitinates Nrf2, leading to degradation of Nrf2 through the 26S proteasome. Nrf2 activation is constitutively maintained at low levels under unstressed conditions. When cells encounter electrophilic or oxidative stresses, cysteine residues of Keap1 are modified and the ubiquitin ligase activity of Keap1 is inactivated. Therefore, Nrf2 is stabilized and accumulates in the nucleus where it binds to antioxidant responsive elements in gene promoters together with small Maf proteins. Intriguingly, cancer cells often manifest high levels of cytoprotection through acquisition of somatic mutations in either the *NRF2* or *KEAP1* gene, which localize in their mutually interacting domains (Padmanabhan *et al.*, 2006; Ohta *et al.*, 2008). These somatic mutations cause a disruption of

the Keap1-Nrf2 binding, resulting in the stabilization and accumulation of Nrf2. Cancer cells with Nrf2 accumulation acquire chemo- and radio-resistance (Wang *et al.*, 2008; Zhang *et al.*, 2010) and metabolic reprogramming toward malignant proliferation (Mitsuishi *et al.*, 2012).

To study the molecular basis of Nrf2 function and the contribution of Nrf2 to cytoprotection against various insults, we have generated *Nrf2* (Itoh *et al.*, 1997) and *Keap1* (Okawa *et al.*, 2006; Taguchi *et al.*, 2010; Wakabayashi *et al.*, 2003) knockout lines of mice. These lines of mice have been used widely and contributed substantially to our understanding of the Keap1-Nrf2 system (Taguchi and Yamamoto 2015). However, there are inherent limitations in the use of mice for toxicological and physiological studies. Rats are a common alternative species for toxicological studies; however, unlike the mouse model, methods to derive and propagate rat embryonic stem (ES) cells were only developed recently (Li *et al.*, 2008), which has restricted severely the use of genetically engineered rats. Although there are many precious natural mutant rats, gene-targeted rats have been largely unavailable. Recent development of a series of genome editing technologies has changed this situation dramatically (Mashimo, 2014). These technologies enable us to generate many gene-knockout model animals simply by using the techniques widely used for the generation of transgenic mice.

With the advent of these gene editing technologies, rats are becoming alternative experimental animals that share many advantages previously associated with genetically engineered murine models (Jacob, 1999). In addition, compared with mice, rats are easier for the conduct of surgeries, provide larger size organs, and offer richer information in behavioral analyses than do mice. One of the most important advantages that rats offer to toxicological studies is reflected in observations that rats appear to mimic the detoxication metabolism of humans more closely than do mice (Wild *et al.*, 1996). Rats are also more suitable for pharmacological studies. Activators of Nrf2 signaling have been developed as therapeutic drugs (Suzuki *et al.*, 2013). Indeed, an Nrf2 activator, dimethyl fumarate (Tecfidera), has been approved for the treatment of multiple sclerosis and many more drug candidates are under development. To validate the efficacy and toxicity of such drugs, rat models are inherently more translational to humans than mouse models.

To initiate the validation of the *Nrf2* knockout rat as a useful tool in understanding toxicological mechanisms and outcomes, we have challenged these animals with aflatoxin B_1 (AFB_1). AFB_1 is a highly carcinogenic mycotoxin produced by *Aspergillus* species of molds. Upon eating foods contaminated with AFB_1, AFB_1 is metabolized in the liver to a reactive epoxide intermediate, AFB_1-8,9-epoxide, by cytochrome P450s (Kensler *et al.*, 2011) and AFB_1-8,9-epoxide spontaneously forms adducts with guanine bases in DNA, resulting in AFB_1-N^7-guanine and AFB_1-formamidopyrimidine. These modified bases elicit DNA mutations. Detoxication of AFB_1 relies on glutathione S-transferases (GSTs) and aldo-keto reductases (AKRs). GSTA3 and/or GSTA5 catalyze conjugation of glutathione to AFB_1-8,9-epoxide and produce AFB_1-glutathione conjugate (AFB_1-SG). AFB_1-SG is sequentially converted to AFB_1-N-acetyl cysteine (AFB_1-NAC) endproduct. Alternatively, the AFB_1-8,9-epoxide is converted to AFB_1-dialdehyde phenolate through an AFB_1-dihydrodiol intermediate. AFB_1-dialdehyde phenolate reacts with proteins such as serum albumin. AFB_1-dialdehyde phenolate is metabolized to AFB_1-dialcohol by AKR7A.

It has been shown that CDDO-Im (2-cyano-3,12-dioxooleana-1,9-dien-28-imidazolide), an Nrf2 activator, protects rats against AFB_1-induced hepatocellular carcinoma with striking potency and efficacy (Johnson *et al.*, 2014). CDDO-Im treatment also decreases the burden of AFB_1-N^7-guanine in liver and increases the elimination of AFB_1-NAC in urine, suggesting that Nrf2 enhances detoxication of AFB_1 *in vivo*. However, further genetic analyses of the mechanisms of protection against AFB_1 toxicity have been hampered because of the lack of *Nrf2* knockout rats. Because mice possess much higher levels of hepatic GST activity toward the AFB_1-epoxide than found in rats and humans (Wild and Turner, 2002), the mouse has not proven to be a suitable model to reproduce AFB_1-induced hepatocellular carcinoma seen in exposed humans. Therefore, in this study, we have undertaken the generation of *Nrf2* knockout rats by means of a genome editing technology and evaluated the impact of disruption of Nrf2 signaling AFB_1 toxicity. We report here that the *Nrf2* knockout rats are informative model animals to evaluate roles that Nrf2 plays in the regulation of AFB_1 detoxication.

MATERIALS AND METHODS

Chemicals

CDDO-Im (2-cyano-3,12-dioxooleana-1,9-dien-28-imidazolide) was generously provided by Mochida Pharmaceutical (Tokyo). AFB_1 (A6636) was purchased from Sigma-Aldrich (St Louis, Missouri). All other chemicals used were obtained from commercial sources and were of the highest grade available.

Animals

Male F344 rats or *Nrf2* knockout C57BL/6J mice (Itoh *et al.*, 1997) were provided water and MR diet (Nosan Co., Kanagawa) *ad libitum*. All rats and mice were maintained under semispecific-pathogen-free conditions and treated according to the regulations of The Standards for Human Care and Use of Laboratory Animals of Tohoku University and Guidelines for Proper Conduct of Animal Experiments of the Ministry of Education, Culture, Sports, Science, and Technology of Japan.

Generation of *Nrf2* Mutant Rats

Generation of *Nrf2* mutant rats followed the standard procedures as described previously (Mashimo *et al.*, 2010). In brief, founder animals heterozygous for deletion of the Nrf2 were generated on F344 inbred background using Zinc finger nuclease (ZFN) technology (Sigma-Aldrich Co.). ZFN constructs were designed to target the upstream of exon 5 in the *Nrf2* sequence, ACCACTGTCCCCAGCCCAgaggccACACTGACAGAG (Figure 1A). Off-target sites with the highest degree of similarity were identified by searching the rat genome (RGSCv3.4) for matches with the ZFN construct sequence with appropriate spacing of 5–6 bp. A list of these target sites is shown in Table 1. Approximately 2–3 pl of ZFN mRNA (10 ng/μl) was injected into the pronuclei of embryos collected from F344/Stm females. The cultured embryos were then transferred to the oviducts of pseudopregnant females (Crlj:WI, 8–10 weeks). A region of exon 5 genomic DNA was then amplified by PCR (94 °C for 30 s, 60 °C for 60 s, 72 °C for 45 s, 35 cycles) using forward primer (Nrf2 Small F: TGAAAATGGGAGTTATCGGG) and reverse primer (Nrf2 Small R: TGTGTTCAAGGTGGGATTTG). The PCR product of the wild-type sample was 334 bp. Amplified samples were then sequenced by ABI3100 (Applied Biosystems) using standard protocols. Each heterozygous pair was maintained to yield littermates of wild-type and homozygous *Nrf2* mutant rats. Toes were clipped and genotyped as shown in Figures 1C and D. All animal care and

experiments conformed to the Guidelines for Animal Experiments of Tohoku University and Kyoto University, and were approved by the Animal Research Committees of Tohoku University and Kyoto University. The resultant rats were deposited to the National BioResource Project for the Rat in Japan (NBRP-Rat) as F344-*Nfe2l2*^{em1Kyo} and F344-*Nfe2l2*^{em2Kyo}.

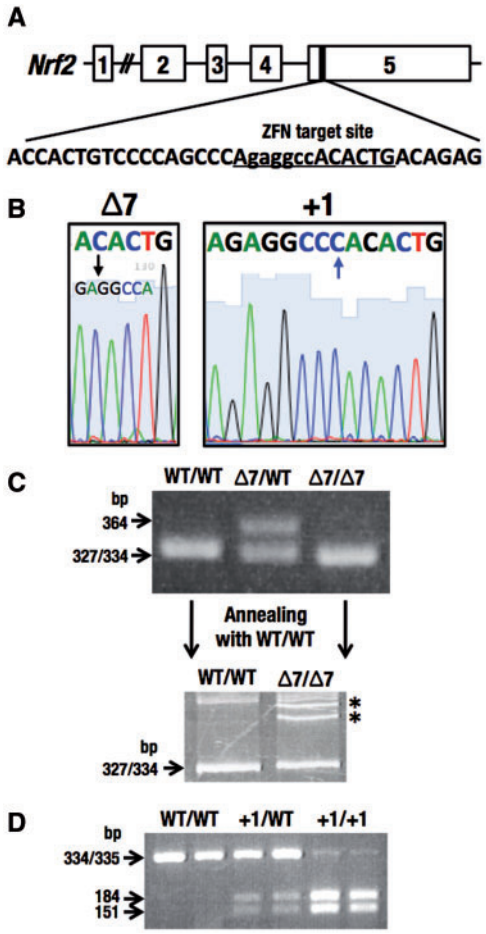

FIG. 1. Generation of *Nrf2* mutant rats. A, The designed target site of zinc finger nuclease (ZFN) in exon 5 of *Nrf2* gene. B, Two lines with an *Nrf2* mutation in the ZFN target site, Δ7 (left) and +1 (right). Sequences underlined in (A) were shown. C, Genotyping of *Nrf2* Δ7 mutation by electrophoresis. Electrophoresis was performed using PCR products in 4% agarose gel (upper panel). The heterozygous sample of Δ7 mutation and wild-type had both 334 and 364 bp. The polyacrylamide gel electrophoresis-based genotyping analysis was analyzed to distinguish a difference between wild-type (334 bp) and Δ7 mutation (327 bp). Annealing and denaturation formed heteroduplex DNA (*), which migrated slower than homoduplex DNA in 9% acrylamide gel (lower panel). D, Genotyping of *Nrf2* +1 mutation by a restriction enzyme, BmgT120I. The PCR product (335 bp) with +1 mutation was digested to 151 and 184 bp by BmgT120I.

Determination of an Intrahepatic Shunt

An intrahepatic shunt was determined by cannulation of the portal vein of 14- to 20-week-old rats, with slight modification to the previous method (Skoko *et al.*, 2014). As a staining solution, bromophenol blue was used instead of trypan blue.

Single Dose of CDDO-Im

Nrf2 knockout rats with Δ7 or +1 mutations and wild-type rats at the age of 6–7 weeks, and wild-type mice and *Nrf2* knockout mice were gavaged with a single dose of an Nrf2 activator, CDDO-Im (30 μmol/kg body weight) or vehicle of 10% cremophor-EL, 10% dimethyl sulfoxide (DMSO) and PBS. Rats and mice were sacrificed 6 h after dosing and the livers harvested.

Single Dose of AFB_1 With or Without CDDO-Im

For detection of the AFB_1-DNA adduct, rats were gavaged with CDDO-Im (30 μmol/kg body weight) 3 times every other day at 8 AM. Twenty-four hours after the last treatment with CDDO-Im, rats were gavaged with 25 μg/100 g body weight of AFB_1 dissolved in DMSO. Rats were then housed in metabolism cages and sacrificed 24 h after the administration of AFB_1. The time schedule is presented in Figure 6A. The serum was analyzed using FUJI DRI-CHEM 7000 (FUJIFILM, Tokyo) to detect alanine transferase (ALT). Livers were immediately frozen in liquid nitrogen using a freeze clamp and stored at −80 °C. DNA was isolated by the method as described (Kensler *et al.*, 1985) and analyzed for levels of AFB_1-DNA adducts by liquid chromatography-mass spectrometry as described previously (Egner *et al.*, 2003). Total DNA content was measured spectrophotometrically using diphenylamine. Immediately following the urine collection, samples were centrifuged at 150 × g and adjusted to an acidic pH using 0.5 mol/l ascorbic acid. Urines were analyzed for levels of AFB_1-N^7-guanine and AFB_1-NAC by isotope dilution mass spectrometry (Egner *et al.*, 2006). Levels were normalized to creatinine content as measured using a spectrophotometric creatinine kit (Eagle Diagnostic), as previously reported (Johnson *et al.*, 2014). Serum AFB_1-adducts were also measured by isotope dilution mass spectrometry as described (Scholl *et al.*, 2006).

Repeated Dose Toxicity of AFB_1 With or Without CDDO-Im

The dose and schedule for administration of CDDO-Im and AFB_1 to rats were identical to that of Yates (Yates *et al.*, 2006). Rats were gavaged with CDDO-Im (30 μmol/kg body weight) for 3 successive weeks on Monday, Wednesday, and Friday at 8 AM. Beginning on the 1 week, AFB_1 (25 μg/rat) was gavaged at 12 AM Monday through Friday for 2 weeks. Rats were sacrificed 5 weeks after the last doses of CDDO-Im and AFB_1. The schedule is presented in Figure 7A.

TABLE 1. Potential ZFN Off-Target Sites

ID	Chr No.	Start Pos.	Sequence[a]	No. of Mismatch	Homodimer (+)/ Heterodimer (−)	Gene
1	chr3	58368282	AACAACTGGAAATAGCCCAAAGATACACTGAGGGAGATGGACA	8	—	—
2	chrX	145527827	AACCAATCTCCTCATCCCCGTTCTACATTGACAGTGATGGAGG	8	—	Hagh
3	chr10	14112775	GGTTCATCTGGGTCTGTGTGTGGTTGGGGTGGGGTCAGAGGGC	8	—	—
4	chr10	109602919	AACCACTGACTGCAGCCAAATGTCACACTGAAAGTTATGGTCT	8	—	—

[a]Bases differing from the consensus target sequence are shown in red. *Fok*I catalytic sequences are shown in green.

TABLE 2. Primers Used in the Quantitative RT-qPCR

Rat Gene	Oligonucleotide Sequence		Reference
Akr7a2	F	5′-GAGCTTGGCTTGTCCAAC-3′	Merrick *et al.* (2012a)
	R	5′-ATCCAGCGGTTGCTTTTA-3′	
Akr7a3	F	5′-CCGCTTCTTTGGGAATCCAT-3′	Hayashi *et al.* (2012)
	R	5′-GGCGATGCCATTGAAGTGT-3′	
Gapdh	F	5′-TTCAATGGCACAGTCAAGGC-3′	Yeligar *et al.* (2010)
	R	5′-TCACCCCATTTGATGTTAGCG-3′	
Gclm	F	5′-CTGCTAAACTGTTCATTGTAGG -3′	Suh *et al.* (2004)
	R	5′-CTATTGGGTTTTACCTGTG -3′	
Gsta3	F	5′-AGTCCTTCACTACTTCGATGGCAG-3′	Djordjevic *et al.* (2015)
	R	5′-CACTTGCTGGAACATCAAACTCC-3′	
Gsta5	F	5′-GTGCAGACCAAAGCCATT-3′	Merrick *et al.* (2012b)
	R	5′-TGAGGGCTCTCTCCTTCA-3′	
Hmox1	F	5′-TTGTCTCTCTGGAATGGAAGG-3′	Yeligar *et al.* (2010)
	R	5′-CTCTACCGACCACAGTTCTG-3′	
Keap1	F	5′-GGACGGCAACACTGATTC-3′	Yamashita *et al.* (2014)
	R	5′-TCGTCTCGATCTGGCTCATA-3′	
Nqo1	F	5′-CATTCTGAAAGGCTGGTTTGA -3′	Yeligar *et al.* (2010)
	R	5′-CTAGCTTTGATCTGGTTGTCA G -3′	

TABLE 3. Antibodies Used in Western Blot

Antibody	Catalog Number	Reference or Company
Anti-AKR7A2	ab175295	Abcam PLC, Cambridge, United Kingdom
Anti-AKR7A3	13209-1-AP	Proteintech Group, Inc., Chicago
Anti-GSTA3		Mclellan *et al.* (1994)
Anti-Keap1	No. 111	Watai *et al.* (2007)
Anti-Lamin B	sc-6217	Santa Cruz Biotechnology Inc., Dallas, Texas
Anti-Nrf2	No. 103	Maruyama *et al.* (2008)
Anti-NQO1	ab2346	Abcam PLC, Cambridge, United Kingdom
Anti-αTubulin	T9026	Sigma-Aldrich Co., LLC, St Louis

Quantitative Reverse Transcription Polymerase Chain Reaction Analysis

Total RNA was isolated from livers using Sepazol-RNA I Super G (Nacalai Tesque, Kyoto). RNA concentration was measured using a NanoDrop 1000 spectrophotometer (Thermo Fisher Scientific, Wilmington, Delaware). RNA was transcribed into cDNA using SuperScript III Reverse Transcriptase (Life Technologies, Carlsbad, California). Reverse transcription-quantitative PCR (RT-qPCR) was performed using the Applied Biosystems ABI7300 PCR system, and thunderbird SYBR qPCR Mix (TOYOBO, Osaka). The data were normalized to *Gapdh* expression. The primers used for RT-qPCR are listed in Table 2.

Microarray Analysis

Total RNA from liver was labeled with Cy3. The samples were hybridized to Oligo DNA Microarray kit for Whole Rat or Mouse Genome (Agilent Technologies, Santa Clara, California) according to the manufacturer's protocol. Arrays were scanned using the G2539A Microarray Scanner System (Agilent Technologies), and the resulting data were analyzed using GeneSpring GX software (Agilent Technologies). The microarray data obtained in this study have been submitted to the Gene Expression Omnibus (GEO) database (http://www.ncbi.nlm.nih.gov/geo/ last accessed April 15, 2016) and assigned the GEO accession number GSE77377. Mouse ChIP-seq data using Nrf2 and MafG antibodies were analyzed (Hirotsu *et al.*, 2012). The samples were mouse Hepa1 cells treated with 100 μM diethylmaleate for 4 h.

Western Blot

Livers were homogenized in 9 volumes of 0.25 M sucrose containing 10 μM MG132, and 10 μM Na_3VO_3, 100 μM NaF and EDTA-free Complete (05056489001, Roche Diagnostics, Germany). Nucleic fraction was isolated as previously reported (Taguchi *et al.*, 2010, 2014). Protein concentration was measured using a bicinchoninic acid protein assay kit (Pierce Biotechnology, Rockford, Illinois), with bovine serum albumin as the standard. The antibodies used for Western blot are listed in Table 3.

Statistical Analysis

The average values were calculated, and the error bars indicate standard deviations. Differences were analyzed using the Student's *t* test. The differences in a survival rate were analyzed using Longrank test. $P < .05$ was considered statistically significant.

RESULTS

Generation of *Nrf2* Mutant Rats Using ZFN Technology

To generate *Nrf2* knockout rats, we designed a ZFN construct that targeted exon 5 (Figure 1A), as we previously had generated an *Nrf2* knockout line of mouse similarly by targeting exon 5 of the mouse *Nrf2* gene (Itoh *et al.*, 1997). To clarify whether the ZFN construct induces mutations only in the targeted region, we have searched for potential off-target sites in the rat genome that are most homologous to the target sequence. We could not find identical target sites in rat genome. Instead, we found 4 sites that carried 8-base mismatches to the on-target site (Table 1). This observation strongly argues that the ZFN construct that we have employed is specific to loci of interest. Although we could not exclude the formal possibility that the ZFN construct might cleave one (or more) of the off-target sites, we surmise that such off-target mutations could be easily

segregated from the Nrf2 locus during the crossing, as the potential off-target sites were located in different chromosomes from the *Nrf2* locus. Therefore, we have concluded that the ZFN construct we have employed is reliable to produce mutant alleles at the locus of interest.

Of the 11 pups obtained from ZFN-injected eggs, 2 pups appeared to be gene-edited in the *Nrf2* locus through mono-allelic mutations. One mutation was a 7-bp deletion (Δ7) and the other was a 1-bp insertion (+1) within the ZFN target site (Figure 1B). Both mutations were expected to produce a truncated Nrf2 protein by introducing stop codons within exon 5. Genotyping analyses of these mutations were conducted by DNA sequencing. For initial genotyping of *Nrf2* Δ7 mutation, we compared the PCR product of 334 bp in the wild-type lane with that of 327 bp in the *Nrf2* Δ7 mutant lane. We found a band at 364 bp appearing in 4% agarose gel electrophoresis in the heterozygote lane (Figure 1C, upper column). The reason for the 364-bp band is a slower running hetero-duplex DNA in agarose gel. As it was technically difficult to identify the 7-bp difference between wild-type and Δ7 mutants by agarose gel electrophoresis (Figure 1C, upper column), we exploited a polyacrylamide gel electrophoresis-based genotyping analysis for the detection of minor differences based on the formation of hetero-duplexes (Zhu *et al.*, 2014). The PCR products (5 μl) with a single band in the agarose gel annealed with the wild-type sample (5 μl) at 72 °C, 5 min and 96 °C, 5 min and maintained at room temperature. The annealing and denaturation processes formed hetero-duplex DNA, which migrated significantly slower than homo-duplex DNA in a 9% polyacrylamide gel (Figure 1C, lower column). The hetero-duplex DNA formed through annealing and denaturation was detected in 4% agarose gel as well as 9% acrylamide gel (data not shown). We reproducibly observed 2 hetero-duplex bands that probably correspond to the hybrids formed by plus and minus complementary strands of amplified wild-type and mutant allele (Espejo *et al.*, 1998).

In contrast, the *Nrf2* +1 mutation resulted in a restriction enzyme-recognition site. The mutation generated a sequence motif that could be cleaved by BmgT120I. Using the restriction fragment length polymorphism assay, the PCR product with +1 mutation (335 bp) was digested to 184- and 151-bp fragments by digestion with BmgT120I (Figure 1D). These multiple approaches enabled us to genotype precisely and reproducibly the 2 *Nrf2* mutations in rats.

Apparent Phenotypes in *Nrf2* Mutant Rats

We have identified 3 unexpected phenotypes in the *Nrf2* knockout mouse; white incisors (Yanagawa *et al.*, 2004), a congenital intrahepatic shunt (Skoko *et al.*, 2014), and smaller liver size (Zhang *et al.*, 2013). Penetration of the incisor and liver size phenotypes are very high, whereas the intrahepatic shunt phenotype is found about half of the mice in C57BL/6J background and much less frequently in ICR background mice.

Although iron deposition makes incisors of rodents red-yellowish, incisors of *Nrf2* knockout mice are whitish, as Nrf2 regulates the genes responsible for iron transport and deposition in the teeth (Yanagawa *et al.*, 2004). In this study, we found that *Nrf2* knockout rats (both with Δ7 and +1 lines) also showed decolorized incisors compared with wild-type rats (Figure 2A), albeit the discoloration was much milder than that in *Nrf2* knockout mice. We also examined the presence of an intrahepatic shunt in the *Nrf2* knockout rats. Our *Nrf2* knockout rats were in the F344 background. Neither the Δ7 nor the +1 mutant showed the presence of apparent shunt, as was the case for the C57BL/6J strain of mouse (Figure 2B). These results suggest that genetic background may play a strong influence on the elaboration of this phenotype. Liver sizes in Δ7 and the +1 mutant were significantly smaller than the littermate wild-type rats (Figure 2B).

Confirmation of Nrf2 Deletion in Rats With Δ7 or +1 Mutations

Nrf2 is constantly degraded by the ubiquitin-proteasome system, and Nrf2 protein is maintained at quite low levels under normal conditions. To verify Nrf2 depletion within the Δ7 and +1 mutants, we administered CDDO-Im to rats in order to induced Nrf2 accumulation (Figure 3A, left panel). Showing very

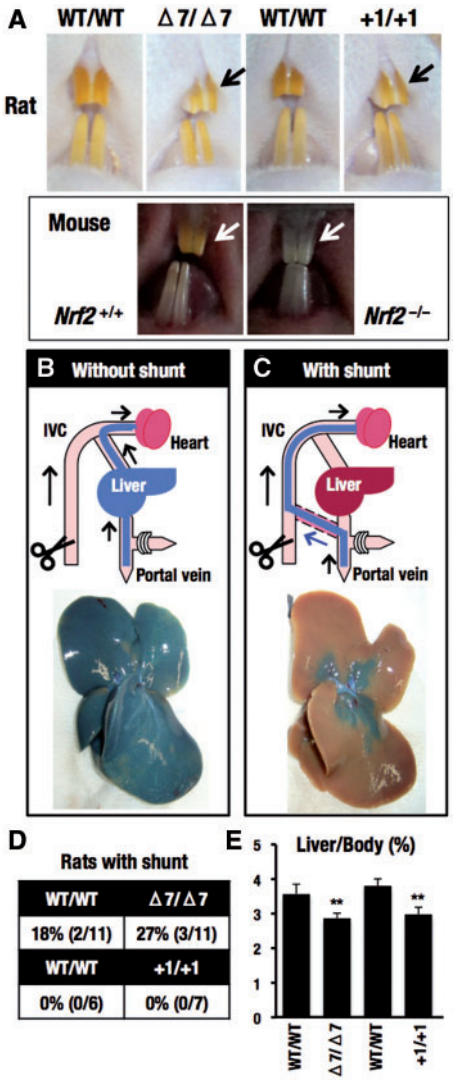

FIG. 2. Comparison of obvious phenotypes between *Nrf2* mutant mice and *Nrf2* mutant rats. *Nrf2* mutant rats with Δ7 or +1 mutations (14–20 weeks old, 6–11 rats) and *Nrf2* knockout mice (11–15 weeks old) were used. A, Color of incisors. Absence (B) or presence (C) of a congenital intrahepatic shunt was determined by cannulation of the portal vein with a catheter, opening of the inferior vena cava and flushing the liver with saline. A solution of bromophenol blue was then perfused into the portal vein. The liver was then excised and photographed. Representative photographs are shown with illustrations. IVC, inferior vena cava. D, Percentages of rats with shunt were calculated. E, Percentages of liver weight to body weight were calculated after injection of bromophenol blue. $^{**}P < .01$.

good agreement with our previous study (Yates *et al.*, 2006), oral administration of CDDO-Im (30 μmol/kg body weight) for 6 h caused nuclear accumulation of Nrf2 in liver of wild-type rats. In contrast, CDDO-Im did not induce Nrf2 accumulation in rats with the Δ7 mutation. Similarly, under basal conditions Nrf2 was completely lost in rats with Δ7 mutations, which is significant when compared with the faint Nrf2 bands in wild-type rats. The loss of Nrf2 induction, as well as loss of basal expression of Nrf2, was quite reproducible in rats with +1 mutations (Figure 3A, right panel). On the other hand, Keap1 protein levels were constant in both wild-type and the Δ7 and +1 mutant rats.

We targeted the last fifth exon of *Nrf2* gene, and in this case nonsense-mediated decay was not expected (Maquat, 2004). The expression of *Nrf2* mRNA levels was comparable with those of the wild-type rats (Figure 3B). Expression levels of *Keap1* mRNA were also constant in all groups, showing very good correlation with the protein levels. In contrast, we found that in Δ7 mutant rats *Ho-1* and *Gclm* mRNAs were not induced by CDDO-Im treatment (Figure 3B). The *Ho-1* and *Gclm* are representative Nrf2 target genes that are usually induced significantly in wild-type rats by CDDO-Im treatment. Indeed, we verified the *Ho-1* and *Gclm* mRNA induction as can be seen in Figure 3B. These changes in *Ho-1* and *Gclm* mRNA expression were quite reproducible in the +1 mutant rats. Collectively, these data demonstrate that the 2 lines rats with Δ7 and +1 mutations in the *Nrf2* gene are genuine *Nrf2* knockout rats, with subsequent loss of the downstream transcriptional activity of Nrf2.

Expression of Nrf2-Target Genes in Microarray Analyses

In order to identify Nrf2-target genes in rats, we performed microarray analyses in which we compared gene expression in *Nrf2* knockout rats with Δ7 or +1 mutations together with CDDO-Im-treated or vehicle-treated wild-type rats. In this analysis, we defined Nrf2-target genes with 2 criteria. First, we selected genes for which levels were induced more than 2-fold in wild-type rats treated with CDDO-Im compared with vehicle-treated wild-type rats. Second, we selected genes with more than 2-fold lower expression in CDDO-Im-treated *Nrf2* knockout rats compared with CDDO-Im-treated wild-type rats.

As shown in Figure 4A, we found 291 probes and 367 pobes of Nrf2-target gene candidates satisfying these 2 criteria in Δ7 and +1 mutant rats, respectively. When we merged these 2 clusters of probes, we found 187 overlapping probes, which corresponded to 106 genes, were commonly induced by CDDO-Im, but the induction was canceled by the mutations in the rat *Nrf2* gene. The genes that were commonly induced in wild-type by CDDO-Im and were canceled by the Δ7 or +1 mutation in the rat

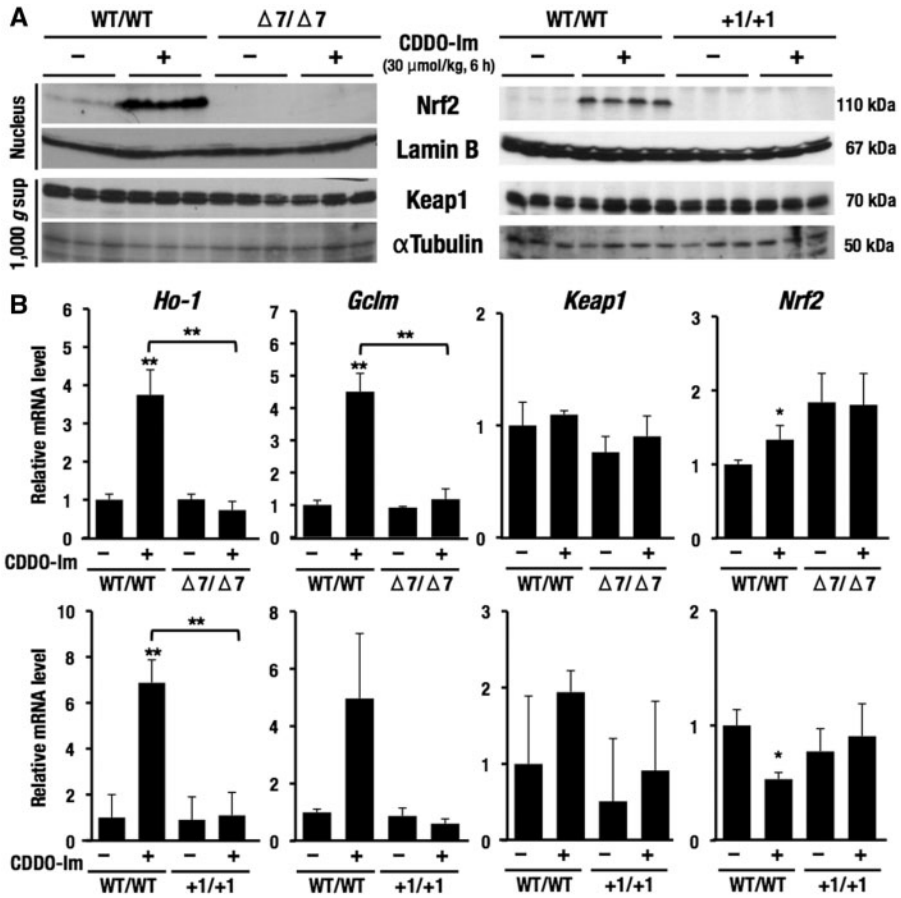

FIG. 3. Confirmation of Nrf2 deletion in *Nrf2* Δ7 or +1 mutations using an Nrf2 activator, CDDO-Im. Single dose of CDDO-Im (30 μmol/kg body weight for 6 h) was orally gavaged to rats. A, Loss of Nrf2 induction by CDDO-Im in the liver of rats with *Nrf2* Δ7 or +1 mutations. Both basal and CDDO-Im-inducible Nrf2 protein expressions in wild-type rats were lost in rats with Δ7 or +1 mutations. Keap1 was expressed constantly in all groups. Lamin B and αTubulin were an internal control in the nucleus and 1000 × g supernatant, respectively. B, Quantification of the mRNA levels in the liver of rats with Δ7 or +1 mutations using RT-qPCR. Nrf2 target genes, *Ho-1* and *Gclm*, were upregulated in CDDO-Im-treated wild-type rats, but not in rats with Δ7 or +1 mutation. *Keap1* was expressed constantly in all groups. *Nrf2* were comparable with those the wild-type rats. *Gapdh* was used as an internal control. The data represent mean ± SD (n = 3–4). $^{**}P < .01$. Asterisks without brackets indicate the comparison with vehicle-treated wild-type rats.

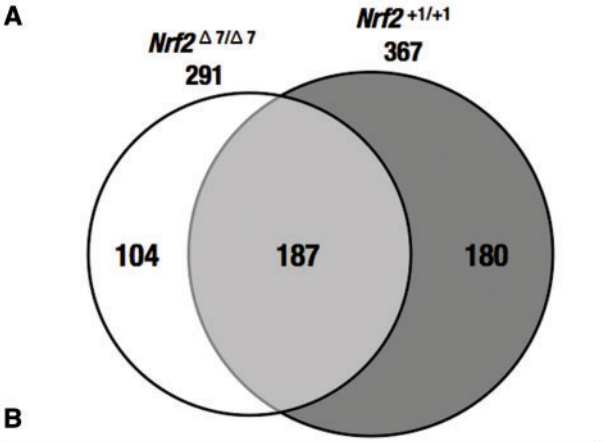

Genes induced by CDDO-Im but the induction was canceled commonly in *Nrf2* Δ7/Δ7 and +1/+1 knockout rats (187 probes = 106 genes)

● *Abcc3*	*Egln3*	*Il17rb*	*Ppm1j*	*Tfap4*
Abcc4	● *Eid3*	*Maff*	*Pprc1*	*Tmem55a*
Akap5	● *Entpd5*	*Mafg*	*Prss22*	*Tmem86a*
● *Akr1b8*	*Epb4.1*	● *Myc*	*Ptgr1*	*Tmprss2*
Akr1b10	*Epha3*	*Ncf2*	*Rassf6*	*Tnrc6a*
Aldh1a7	*G6pdx*	*Nle1*	*Ropn1*	*Trib3*
● *Ampd3*	*Gch1*	*Nol8*	*Rpp38*	● *Trim16*
Bach1	● *Gclc*	*Nop56*	*Rrs1*	*Trmt61a*
Bcat2	● *Gclm*	*Nop58*	● *Samd4*	*Tubb3*
Bex1	*Gjb2*	● *Nqo1*	*Slc1a4*	● *Txnrd1*
Car2	● *Gnat1*	*Nrg1*	*Slc7a1*	● *Uchl1*
Ccdc158	*Gpatch4*	*Ntrk1*	*Slc7a11*	● *Ugdh*
Cd3eap	● *Gpx2*	*Nudt10*	*Slc15a1*	*Wdr43*
Cdk6	*Grhl1*	● *Nudt11*	*Slc25a37*	*Ydjc*
Clcf1	*Gsta3*	● *Pir*	● *Slc35e3*	*Zdhhc7*
Coro6	*Gtf2h1*	*Pla2g7*	*Snx10*	*Zfand2a*
Creg1	*Hmgcr*	*Pla2g12a*	*Spsb1*	● *Zfp418*
Cryl1	● *Hmox1*	● *Plk3*	● *Srxn1*	*Zfp593*
Csmd1	*Hpdl*	*Polr1e*	*Ssmem1*	*BC055111*
Disp1	*Htatip2*	*Polr3g*	*Tex21*	*D330045A20Rik*
Dus4l	*Ier3*	*Ppan*	*Tex36*	*2010300C02Rik*
				4933422H20Rik

53 genes that are identified in mouse ChIP-seq analyses with both Nrf2 and MafG antibodies

● 23 genes that are induced in mice by CDDO-Im but the induction was canceled by the *Nrf2* gene knockout

FIG. 4. Nrf2-dependent gene induction by CDDO-Im. Microarray analyses were performed using wild-type rats and rats with *Nrf2* Δ7 or +1 mutations in the absence or presence CDDO-Im. In this analysis, we defined Nrf2-target genes with 2 criteria. First, we selected genes whose levels were induced more than 2-fold in wild-type rats treated with CDDO-Im compared with that in vehicle-treated wild-type rats. Second, we selected genes downregulated more than 2-fold in CDDO-Im-treated *Nrf2* knockout rats compared with CDDO-Im-treated wild-type rats. Number (A) and names (B) of the genes that were induced by CDDO-Im but for which induction was canceled by the *Nrf2* Δ7 or +1 mutation. The 187 probes correspond to 106 genes. Fifty-three genes marked by shadowing were in common with the mouse genes to which both Nrf2 and MafG bound in ChIP-seq analyses (Hirotsu *et al.*, 2012). Twenty-three genes with black dots were found to show Nrf2-dependent induction by CDDO-Im in a similar set of analyses in which wild-type and *Nrf2* knockout mice were treated with CDDO-Im under the same condition as that used for rats.

Nrf2 gene are listed in Figure 4B. This group of genes included ATP-binding cassette (ABC) transporters (*Abcc3*, *Abcc4*), aldo-keto reductase (AKR) family (*Akr1b8*, *Akr1b10*), aldehyde dehydrogenase (ALDH) family (*Aldh1a7*), transcription factors (*Bach1*, *Myc*), glutathione synthetase (*Gclc*, *Gclm*), GST family (*Gsta3*), antioxidative enzymes (*Gpx2*, *Hmox1*, *Nqo1*, *Slc7a11*, *Srxn1*, *Txnrd1*), small Maf (*Maff*, *Mafg*), and a metabolic enzyme (*G6pdx*). These genes have been shown to be Nrf2-target genes in various gene expression analyses using mouse and human cells. For instance, the inductions of *Hmox1* (named as *Ho-1*) and *Gclm* by CDDO-Im were indeed suppressed in *Nrf2* knockout rats with Δ7 and +1 mutations (see Figure 3B). To our surprise, however, only 23 genes were found commonly in mice that were induced by CDDO-Im and the induction was canceled by the *Nrf2* gene knockout in the same experimental condition as that employed for rats. Showing very good agreement, only 53 genes of the 106 genes identified in rats were found in the positive gene data of mouse Nrf2 and MafG ChIP-seq analyses (Hirotsu *et al.*, 2012). Even considering the differences in experimental conditions, these results imply the significant genetic variations in the regulation of detoxifying enzymes between these 2 species.

Nrf2-Dependent Detoxication of AFB_1

As shown in Figure 5A, AFB_1 is metabolized to AFB_1-8,9-epoxide by cytochrome P450s. AFB_1-8,9-epoxide is then conjugated with glutathione by GSTA3 and GSTA5 or is converted to AFB_1-dihydrodiol by hydrolysis. In the acidic condition, AFB_1-dihydrodiol is converted to AFB_1-dialdehyde phenolate, which is metabolized to AFB_1-dialcohol by AKR7A2 and AKR7A3. Thus, GST and AKR isozymes are important for detoxication of AFB_1.

Using the *Nrf2* knockout rats under the same conditions as for the data depicted in Figure 3, we examined whether enzymes responsible for detoxication of AFB_1 were expressed in an Nrf2-dependent manner or not. The basal expression of GSTA3, AKR7A2, and AKR7A3 was decreased reproducibly in both lines of *Nrf2* knockout rats compared with wild-type rats (Figure 5B), demonstrating the Nrf2-dependency in the induction of these gene transcripts. The expression of mRNAs related to detoxication of AFB_1 (*Gsta3*, *Gsta5*, *Akr7a2*, and *Akr7a3*) was also examined (Figure 5C). CDDO-Im elevated expression of these mRNAs in wild-type rats, but not in *Nrf2* knockout rats, indicating that the expression of these genes is Nrf2-dependent. *Gsta3* was also identified as an Nrf2-depenent gene by microarray analyses as shown in Figure 4B.

Nrf2 Is Protective Against AFB_1 Toxicity in Liver

In order to quantify potential modulation of levels of DNA or protein adducts following administration of AFB_1 (see Figure 5A), single doses of AFB_1 with or without prior CDDO-Im treatments were administered to the 4 groups of rats. The schedule for dosing with AFB_1 and CDDO-Im is shown in Figure 6A and treatment assignments for the groups of rats are shown in Figure 6B. As shown in Figure 6C, simultaneous administration of CDDO-Im gave rise to the enlargement of livers in AFB_1-treated wild-type rats (group 2) compared with vehicle-treated wild-type rats (group 1). In *Nrf2* knockout rats with Δ7 mutation (groups 3 and 4), liver sizes were significantly smaller than wild-type rats, and the CDDO-Im treatment made no difference.

The AFB_1-treatment increased serum ALT levels, a marker of liver injury, of wild-type rats, but ALT levels remained at normal levels with pretreatment with CDDO-Im (Figure 6D). These results are consistent with the previous observation that CDDO-Im is protective against AFB_1 toxicity (Johnson *et al.*, 2014). Importantly, the AFB_1-treatment significantly increased ALT levels in *Nrf2* knockout rats with Δ7 mutation compared with wild-type rats; however, pretreatment of CDDO-Im did not afford significant protection (Figure 6D). These results indicate that Nrf2 is an important determinant of the extent of hepatotoxicity of AFB_1, and that CDDO-Im exerts protective effects through Nrf2 signaling.

To verify this notion, we quantified metabolites that are indicators of toxicity and detoxication of AFB_1. As described earlier,

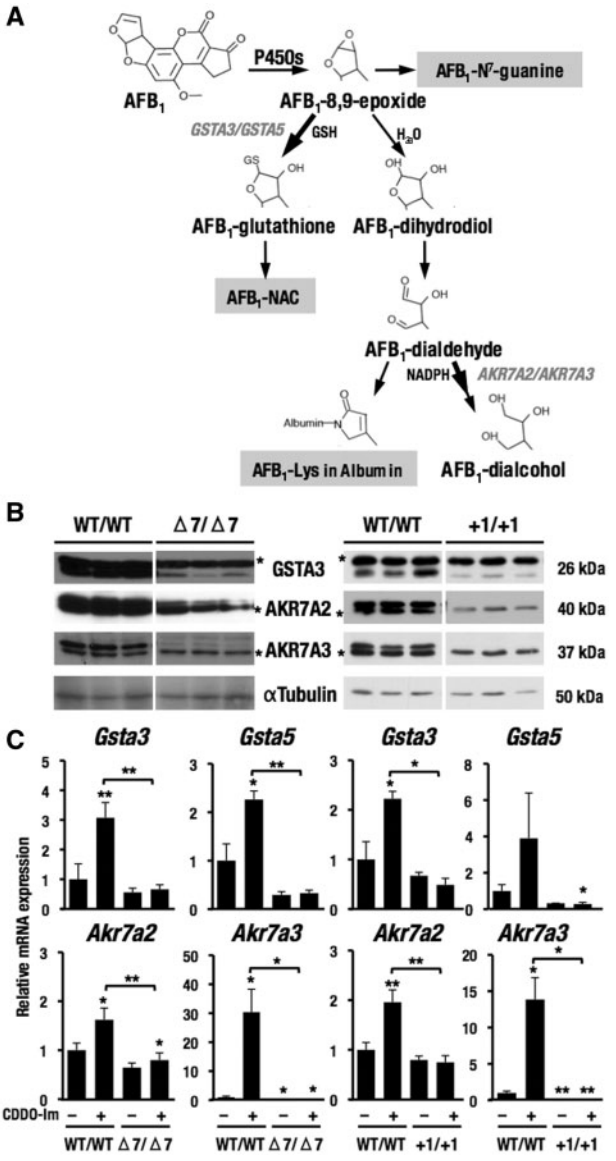

FIG. 5. Nrf2-dependent basal expression of enzymes responsible for AFB_1 detoxication. A, The metabolic pathway of AFB_1. B, Expression of enzymes responsible for AFB_1 detoxication in *Nrf2* knockout rats with Δ7 or +1 mutations. αTubulin was an internal control in the cytoplasmic fraction. *Nonspecific band. C, mRNA expression of genes related to AFB_1 detoxication. The data represent mean ± SD (n = 3–4). *$P < .05$; **$P < .01$. Asterisks without brackets indicate the comparison with vehicle-treated, wild-type rats.

the reactive metabolite AFB_1-8,9-epoxide is detoxified either by glutathione conjugation or by hydration followed by further reduction through AKRs. In the latter case, resulting AFB_1-dialdehyde reacts with proteins, such as serum albumin. Urine volumes were not affected in the 4-genotype groups (Figure 6E). We found that CDDO-Im decreased significantly the AFB_1-N^7-guanine levels isolated from liver DNA and excreted into urine of AFB_1-treated wild-type rats (Figure 6F). CDDO-Im-treatment enhanced the urinary levels of AFB_1-NAC, but did not significantly reduce levels of AFB_1-Lys in serum. The former is an ultimate metabolite of AFB_1-glutathione conjugate, whereas the latter is a product of AFB_1-albumin interaction (see Figure 5A).

Levels of AFB_1-N^7-guanine were increased in both the liver and urine of *Nrf2* knockout rats with Δ7 mutation. AFB_1-NAC in urine and AFB_1-Lys in serum of *Nrf2* knockout rats with Δ7 mutation did not show significant differences from those of wild-type rats. The CDDO-Im pretreatment did not affect levels of these 3 metabolites, demonstrating that the protective alterations in the detoxication of AFB_1 seen in wild-type rats do not occur in the *Nrf2* knockout rats.

Nrf2 Knockout Rats Are Sensitive to AFB_1 Toxicity

Our analyses of rats with a single AFB_1 injection revealed that Nrf2 is critical for protection against the acute toxicity of AFB_1. To ascertain this point further, we conducted subchronic injections of AFB_1 to the *Nrf2* knockout rats. The protocol of this experiment is shown in Figure 7A. *Nrf2* knockout rats with Δ7 mutation did not gain body weight during the periods of administration of AFB_1 (5 days in each week), but did gain weight during the 2-day dosing holiday and after AFB_1 dosing stopped (Figure 7B). Co-treatment of CDDO-Im did not affect the ratios of body weight gain of both the AFB_1-treated wild-type and *Nrf2* knockout rats.

Strikingly, more than a half of the *Nrf2* knockout rats (5/8 rats; 62.5%) died following AFB_1 treatment (Figure 7C). Concomitant treatment of CDDO-Im did not protect the *Nrf2* knockout rats against the toxicity of AFB_1 (4/6 rats; 66.7%). The dose of AFB_1 employed was not toxic for the wild-type rats. Body weights of the surviving *Nrf2* knockout rats were almost similar to those of the wild-type rats. Based on the results shown in Figure 6 (metabolism) and Figure 7 (survival), we conclude that *Nrf2* knockout rats are highly sensitive to AFB_1 toxicity due to impaired capacity for AFB_1 detoxication.

DISCUSSION

Nrf2 has been emerging as a key transcription factor that regulates expression of genes of cytoprotective enzymes. Especially in the field of toxicology, *Nrf2* knockout mice have been serving as an excellent model system to examine physiological and pathological regulation of enzymes involved in detoxication pathways (Itoh *et al.*, 1997; Taguchi *et al.*, 2011). Genetic activation of Nrf2 by *Keap1* knockout or knockdown gives rise to an elaborate counterpoint to the *Nrf2* knockout mice (Okawa *et al.*, 2006; Taguchi *et al.*, 2010; Wakabayashi *et al.*, 2003). Aberrant Nrf2 activation caused by somatic mutations of *Keap1* or *Nrf2* genes in a variety of cancers (Padmanabhan *et al.*, 2006; Singh *et al.*, 2006) appears to be linked to emergence of resistant foci toward insults of toxic chemicals (Solt *et al.*, 1977). In this study, we established *Nrf2* knockout rats as an additional, more facile model system for toxicological studies. We have generated and characterized 2 lines of *Nrf2* knockout rats, and found that the *Nrf2* knockout rats share many common phenotypes with the *Nrf2* knockout mouse. Using the *Nrf2* knockout rats, we examined a protective role that Nrf2 plays against toxic chemicals. These *Nrf2* knockout rats broaden the opportunities for molecular toxicology in the species *Rattus*.

As an experimental model animal, rats have provided historically a number of important physiological, pathological, or toxicological insights. For instance, a number of naturally occurring mutant rats related to diseases are available; Dahl rats for susceptibility (S rat) or resistance (R rat) to salt-induced hypertension (Dahl *et al.*, 1962), Goto-Kakizaki rat for type 2 diabetes (Goto *et al.*, 1975), HRSP rats for stroke-prone spontaneous hypertension (Yamori *et al.*, 1976), Tremor rat for Canavan disease (Yamada *et al.*, 1985), and Zitter rat for spongiform encephalopathy (Kondo *et al.*, 1993). Rats have been considered a better

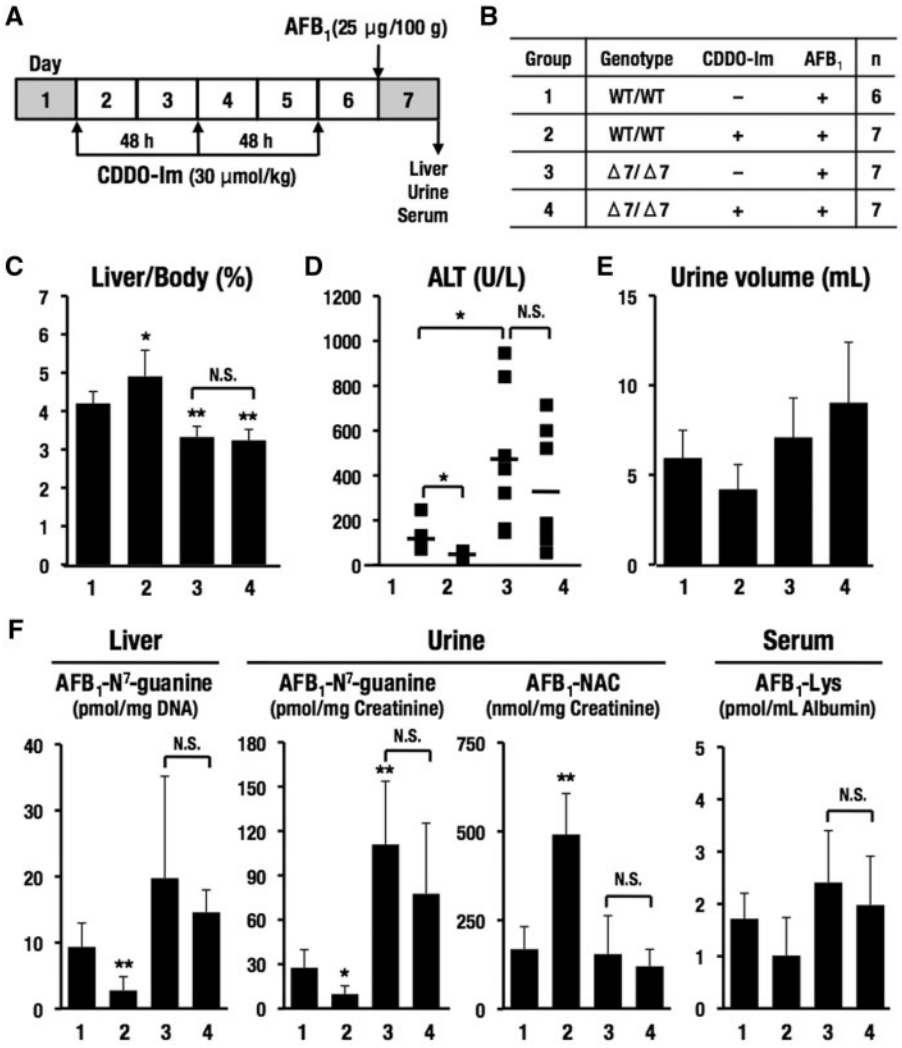

FIG. 6. Effects of a single dose of AFB_1 with CDDO-Im in wild-type rats and *Nrf2* knockout rats with Δ7 mutation. A, Schedule of treatment of CDDO-Im and AFB_1. Rats were gavaged with CDDO-Im (30 μmol/kg body weight) 3 times every other day at 8 AM. Twenty-four hours after the last treatment with CDDO-Im, rats were gavaged with AFB_1 (25 μg/100 g body weight). Rats in metabolic cages at days 1 and 7 were sacrificed 24 h after administration of AFB_1. B, Groups of genotypes and treatments. Rats (200–265 g on the first day of administration of CDDO-Im) were used. C, Percentages of liver to body weight. D, Serum ALT. E, Urine volume. F, Metabolites of AFB_1 in the liver, urine, and serum. The data represent mean ± SD (n = 6–7). $^*P < .05$; $^{**}P < .01$. Asterisks without brackets indicate the comparison with group 1.

model animal than mice for toxicological studies because of size, ease of handling, lower background rates of neoplasia, and other intrinsic factors. Notably, their metabolic pathways appear to share much more similarity to humans than do those of mice. However, one problem that places the rat system behind of the mouse system for molecular toxicology studies is the difficulty to prepare ES cells, which are essential for gene targeting. Until very recently methods to derive and propagate rat ES cells were not available (Li *et al.*, 2008), so that engineering for genome modified rats was not possible. A striking breakthrough was the recent introduction of genome editing technologies, including ZFN, TALEN and CRISPR/Cas, which assure deletion of rat genes or precision knock-in of transgenes at specific sites in the rat genome to produce conditional knockout rats without the use of ES cells (Mashimo *et al.*, 2010).

As systematic or conditional knockout mice of both *Nrf2* and *Keap1* have been generated, the mouse system has been served as a powerful analytical tool to examine the Keap1-Nrf2 system *in vivo*. This situation will be sustained into the future. However, some of the limitations of the mouse system will be overcome by the use of other animals, and rats appear to be the front-runner choice. In the toxicological field, aryl hydrocarbon receptor (AhR) (Fujii-Kuriyama and Mimura, 2005) and Nrf2 are 2 important transcription factors that regulate expression of the phase I and phase II detoxication enzymes, respectively. Recently, *AhR* knockout line of rats was reported by using Sprague Dawley (SD) outbred background using ZFN technology (Harrill *et al.*, 2013). Quite recently, as an independent attempt from this study, *Nrf2* knockout line of rats has been generated in SD background using TALEN technology for analysis of the pathophysiology of hypertension (Priestley *et al.*, 2015). Our *Nrf2* knockout lines of rats use the F344 strain for which there is a wealth of published toxicological information and foresee these animals as useful tools in toxicological research, especially as a new model animal for Keap1-Nrf2 studies. In Figure 3, we listed the rat genes that were induced by CDDO-Im in wild-type F344 rats, but where the induction was blunted by the Nrf2 mutations. Many of such Nrf2-dependent genes identified in rats were found to be responsible for detoxication and anti-oxidative responses. However, the profile of the Nrf2-dependent genes is

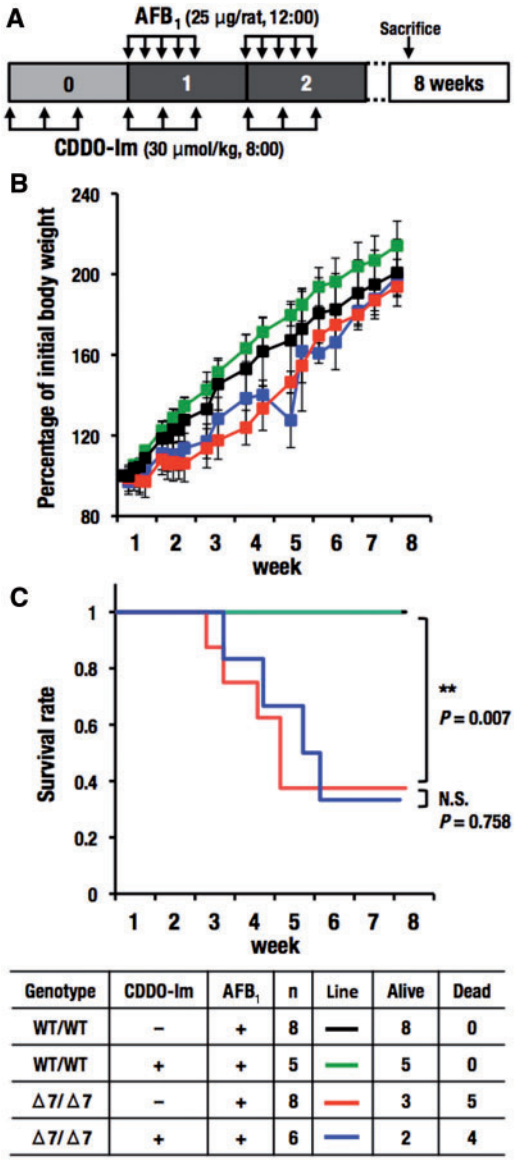

Genotype	CDDO-Im	AFB_1	n	Line	Alive	Dead
WT/WT	–	+	8		8	0
WT/WT	+	+	5		5	0
Δ7/Δ7	–	+	8		3	5
Δ7/Δ7	+	+	6		2	4

FIG. 7. Effects of repeated doses of AFB_1 with CDDO-Im in wild-type and *Nrf2* knockout rats with Δ7 mutation. A, Schedule of treatment of CDDO-Im and AFB_1. Rats were gavaged with CDDO-Im (30 μmol/kg body weight) for 3 successive weeks on Monday, Wednesday, and Friday at 8 AM. Beginning on the first week, AFB_1 (25 μg/rat) was gavaged at 12 AM Monday through Friday for 2 weeks. Rats were sacrificed 5 weeks after the last doses of CDDO-Im and AFB_1. B, Change of body weight. Rats (104–168 g on the first day of administration of AFB_1) were used. Body weight on the first day of administration of AFB_1 was set to 100%. The data represent mean ± SD (n = 5–8). C, Survival rate. Four groups were listed in the table. $^{**}P < .01$. Asterisks with brackets indicate the comparison between indicated groups.

fairly divergent when compared with that of mice, conforming the previous observation that the detoxification genes in these species are substantially different (Wild and Turner, 2002).

As a prelude to the broader use of these animals in toxicological research, we have characterized the effect of Nrf2 disruption on the toxicity and disposition of AFB_1. Rats, unlike mice, are sensitive to the carcinogenic actions of this mycotoxin. However, there have been limited opportunities to use genetically engineered animals to probe the key determinants of sensitivity or resistance. AFB_1 exerts carcinogenic effects through its bioactivation. As presented in Figure 5A, the reactive metabolite AFB_1-8,9-epoxide binds to DNA to form AFB_1-N^7-guanine. Therefore, AFB_1-N^7-guanine and AFB_1-Lys in albumin are biomarkers of AFB_1 toxicity. On the other hand, GSTs and AKRs are essential for the detoxication of AFB_1 metabolites. A transgenic rat harboring AKR7A1 (human AKR7A3), which enhances detoxication of a reactive metabolite AFB_1-dialdehyde, was utilized to examine protection against acute and chronic AFB_1 toxicity (Roebuck *et al.*, 2009). Overexpression of AKR7A3 increased formation of AFB_1-alcohols in liver and urine. However, the AKR7A3 transgenic rats appeared not to protect against the formation of GST-P-positive preneoplastic foci upon chronic exposure to AFB_1, implying that the prevention of protein-adduct formation mediated by AKR was not a critical process for protection against AFB_1 tumorigenicity. Therefore, the results of AKR7A3 transgenic mice indicate by inference that a glutathione conjugation of AFB_1-8,9-epoxide by GSTs is a primary detoxication reaction.

A *Gsta3* knockout mouse was utilized to examine whether glutathione conjugation is essential for detoxication of AFB_1 (Kensler *et al.*, 2014). As expected, hepatic AFB_1-N^7-guanine level and urinary excretion of AFB_1-N^7-guanine were both elevated in the *Gsta3* knockout mice compared with those of wild-type mice. In contrast, urinary excretion of AFB_1-NAC was much lower in *Gsta3* knockout mouse than in wild-type mice. In addition, Nrf2 activation by CDDO-Im administration or Keap1 deletion did not rescue *Gsta3* knockout mouse from the genotoxicity. These results indicate that GSTA3 is responsible for the detoxication of AFB_1 in mice. Cross-species comparisons indicate that humans and rats form similar levels of AFB_1-Lys in albumin upon AFB_1 exposure, but in contrast mice and hamsters form far less AFB_1-Lys (Wild *et al.*, 1996). In addition to the intrinsic resistance to the hepatocarcinogenicity of AFB_1, these wide ranging results suggest that mouse may not be a suitable animal model for the study of AFB_1 toxicity.

It is intriguing to note the recent finding using the "Solt-Farber" protocol for induction of hepatocellular carcinoma in rats (Zavattari *et al.*, 2015). This protocol utilizes a combination of diethyl-nitrosamine and 2-acetaminofluorene, followed by a partial hepatectomy (Solt *et al.*, 1977). In the Solt-Farber model, somatic mutations in either *Nrf2* or *Keap1* genes are found in 71% of GST-P-positive early preneoplastic lesions (Zavattari *et al.*, 2015). Missense mutations of *Nrf2* are more frequent than those of *Keap1*. Importantly, the *Nrf2* somatic mutations are located in DLG and ETGE motifs, which are 2 independent Keap1-binding motifs of Nrf2, consistent with the observations in lung and esophagus cancers (Fukutomi *et al.*, 2014). These observations suggest that Nrf2 is critical for the progression and development of hepatocellular carcinomas in the Solt-Farber model. In fact, *Gstp* is an Nrf2 target gene, and its product GST-P has been shown as a representative marker for the preneoplastic lesions, both in this model and following treatment with AFB_1. However, there remain many unsolved questions in regards to the Nrf2 contribution to hepatocellular carcinogenesis. For instance, how Nrf2 and Keap1 acquire such frequent somatic mutations in the preneoplastic lesions of Solt-Farber model and other hepatocarcinogenic protocols or which oncogenes or anticancer genes are responsible for carcinogenesis under Nrf2 regulation are not known. We believe that the *Nrf2* knockout rat may be a very powerful tool for the elucidation of these issues.

In conclusion, in this study we have generated *Nrf2* knockout rats by means of a genome editing technology. We report here that the *Nrf2* knockout rat is a useful animal model to evaluate the roles that Nrf2 plays in modulating AFB_1 detoxication and

toxicity and will have broad application to molecular toxicology studies with many agents and processes of interest to the field.

ACKNOWLEDGMENTS

The authors thank Professor John Hayes (Dundee University, United Kingdom) for anti-GSTA3 antibodies and precious advice, Mochida Pharmaceutical Co. Ltd. for generous supply of CDDO-Im, and the Biomedical Research Core of Tohoku University Graduate School of Medicine for technical support.

FUNDING

MEXT/JSPS KAKENHI (24249015, 26111002, and 15H02507 to M.Y., 24790307, 25117703, and 26460384 to K.T.); AMED-CREST, AMED (to M.Y.); MEXT [a research program of the Project for Development of Innovative Research on Cancer Therapeutics (P-Direct)]; the Mitsubishi Foundation, and the Takeda Science Foundation (to M.Y.); the Gushinkai Foundation and Gonryo Medical Foundation (to K.T.); the Naito Foundation (to K.T. and M.Y.); the U.S. National Institutes of Health R35 CA197222 (to T.W.K.).

REFERENCES

Dahl, L. K., Heine, M., and Tassinari, L. (1962). Effects of chronic excess salt ingestion - evidence that genetic factors play an important role in susceptibility to experimental hypertension. *J. Exp. Med.* **115**, 1173–1190.

Djordjevic, J., Djordjevic, A., Adzic, M., Mitic, M., Lukic, I., and Radojcic, M. B. (2015). Alterations in the Nrf2-Keap1 signaling pathway and its downstream target genes in rat brain under stress. *Brain Res.* **1602**, 20–31.

Egner, P. A., Groopman, J. D., Wang, J. S., Kensler, T. W., and Friesen, M. D. (2006). Quantification of aflatoxin-B1-N7-Guanine in human urine by high-performance liquid chromatography and isotope dilution tandem mass spectrometry. *Chem. Res. Toxicol.* **19**, 1191–1195.

Egner, P. A., Yu, X., Johnson, J. K., Nathasingh, C. K., Groopman, J. D., Kensler, T. W., and Roebuck, B. D. (2003). Identification of aflatoxin M1-N7-guanine in liver and urine of tree shrews and rats following administration of aflatoxin B1. *Chem. Res. Toxicol.* **16**, 1174–1180.

Espejo, R. T., Feijoo, C. G., Romero, J., and Vasquez, M. (1998). PAGE analysis of the heteroduplexes formed between PCR-amplified 16S rRNA genes: Estimation of sequence similarity and rDNA complexity. *Microbiol-Uk* **144**, 1611–1617.

Fujii-Kuriyama, Y., and Mimura, J. (2005). Molecular mechanisms of AhR functions in the regulation of cytochrome P450 genes. *Biochem. Bioph. Res. Commun.* **338**, 311–317.

Fukutomi, T., Takagi, K., Mizushima, T., Ohuchi, N., and Yamamoto, M. (2014). Kinetic, thermodynamic, and structural characterizations of the association between Nrf2-DLGex degron and Keap1. *Mol. Cell. Biol.* **34**, 832–846.

Goto, Y., Kakizaki, M., and Masaki, N. (1975). Spontaneous diabetes produced by selective breeding of normal wistar rats. *Proc. Jpn. Acad.* **51**, 80–85.

Harrill, J. A., Hukkanen, R. R., Lawson, M., Martin, G., Gilger, B., Soldatow, V., LeCluyse, E. L., Budinsky, R. A., Rowlands, J. C., and Thomas, R. S. (2013). Knockout of the aryl hydrocarbon receptor results in distinct hepatic and renal phenotypes in rats and mice. *Toxicol. Appl. Pharm.* **272**, 503–518.

Hayashi, H., Shimamoto, K., Taniai, E., Ishii, Y., Morita, R., Suzuki, K., Shibutani, M., and Mitsumori, K. (2012). Liver tumor promoting effect of omeprazole in rats and its possible mechanism of action. *J. Toxicol. Sci.* **37**, 491–501.

Hirotsu, Y., Katsuoka, F., Funayama, R., Nagashima, T., Nishida, Y., Nakayama, K., Engel, J. D., and Yamamoto, M. (2012). Nrf2-MafG heterodimers contribute globally to antioxidant and metabolic networks. *Nucleic Acids Res.* **40**, 10228–10239.

Itoh, K., Chiba, T., Takahashi, S., Ishii, T., Igarashi, K., Katoh, Y., Oyake, T., Hayashi, N., Satoh, K., Hatayama, I., *et al.* (1997). An Nrf2/small Maf heterodimer mediates the induction of phase II detoxifying enzyme genes through antioxidant response elements. *Biochem. Biophys. Res. Commun.* **236**, 313–322.

Jacob, H. J. (1999). Functional genomics and rat models. *Genome Res.* **9**, 1013–1016.

Johnson, N. M., Egner, P. A., Baxter, V. K., Sporn, M. B., Wible, R. S., Sutter, T. R., Groopman, J. D., Kensler, T. W., and Roebuck, B. D. (2014). Complete protection against aflatoxin B(1)-induced liver cancer with a triterpenoid: DNA adduct dosimetry, molecular signature, and genotoxicity threshold. *Cancer Prev. Res. (Phila)* **7**, 658–665.

Kensler, K. H., Slocum, S. L., Chartoumpekis, D. V., Dolan, P. M., Johnson, N. M., Ilic, Z., Crawford, D. R., Sell, S., Groopman, J. D., Kensler, T. W., and., *et al.* (2014). Genetic or pharmacologic activation of nrf2 signaling fails to protect against aflatoxin genotoxicity in hypersensitive gsta3 knockout mice. *Toxicol. Sci.* **139**, 293–300.

Kensler, T. W., Egner, P. A., Trush, M. A., Bueding, E., and Groopman, J. D. (1985). Modification of aflatoxin B1 binding to DNA in vivo in rats fed phenolic antioxidants, ethoxyquin and a dithiothione. *Carcinogenesis* **6**, 759–763.

Kensler, T. W., Roebuck, B. D., Wogan, G. N., and Groopman, J. D. (2011). Aflatoxin: a 50-year odyssey of mechanistic and translational toxicology. *Toxicol. Sci.* **120 Suppl 1**, S28–S48.

Kobayashi, A., Kang, M. I., Okawa, H., Ohtsuji, M., Zenke, Y., Chiba, T., Igarashi, K., and Yamamoto, M. (2004). Oxidative stress sensor Keap1 functions as an adaptor for Cul3-based E3 ligase to regulate proteasomal degradation of Nrf2. *Mol. Cell. Biol.* **24**, 7130–7139.

Kondo, A., Sendoh, S., Takamatsu, J., and Nagara, H. (1993). The zitter rat: membranous abnormality in the Schwann cells of myelinated nerve fibers. *Brain Res.* **613**, 173–179.

Li, P., Tong, C., Mehrian-Shai, R., Jia, L., Wu, N., Yan, Y., Maxson, R. E., Schulze, E. N., Song, H., Hsieh, C. L., *et al.* (2008). Germline competent embryonic stem cells derived from rat blastocysts. *Cell* **135**, 1299–1310.

Maquat, L. E. (2004). Nonsense-mediated mRNA decay: splicing, translation and mRNP dynamics. *Nat. Rev. Mol. Cell. Biol.* **5**, 89–99.

Maruyama, A., Tsukamoto, S., Nishikawa, K., Yoshida, A., Harada, N., Motojima, K., Ishii, T., Nakane, A., Yamamoto, M., and Itoh, K. (2008). Nrf2 regulates the alternative first exons of CD36 in macrophages through specific antioxidant response elements. *Arch. Biochem. Biophys.* **477**, 139–145.

Mashimo, T. (2014). Gene targeting technologies in rats: zinc finger nucleases, transcription activator-like effector nucleases, and clustered regularly interspaced short palindromic repeats. *Dev. Growth Differ.* **56**, 46–52.

Mashimo, T., Takizawa, A., Voigt, B., Yoshimi, K., Hiai, H., Kuramoto, T., and Serikawa, T. (2010). Generation of knockout rats with X-Linked severe combined immunodeficiency (X-SCID) using zinc-finger nucleases. *PLoS One* **5**,

Mclellan, L. I., Judah, D. J., Neal, G. E., and Hayes, J. D. (1994). Regulation of aflatoxin B-1-metabolizing aldehyde reductase

and glutathione-S-transferase by chemoprotectors. *Biochem. J.* **300**, 117–124.

Merrick, B. A., Auerbach, S. S., Stockton, P. S., Foley, J. F., Malarkey, D. E., Sills, R. C., Irwin, R. D., and Tice, R. R. (2012a). Testing an aflatoxin B1 gene signature in rat archival tissues. *Chem. Res. Toxicol.* **25**, 1132–1144.

Merrick, B. A., Auerbach, S. S., Stockton, P. S., Foley, J. F., Malarkey, D. E., Sills, R. C., Irwin, R. D., and Ticet, R. R. (2012b). Testing an aflatoxin B1 gene signature in rat archival tissues. *Chem. Res. Toxicol.* **25**, 1132–1144.

Mitsuishi, Y., Taguchi, K., Kawatani, Y., Shibata, T., Nukiwa, T., Aburatani, H., Yamamoto, M., and Motohashi, H. (2012). Nrf2 redirects glucose and glutamine into anabolic pathways in metabolic reprogramming. *Cancer Cell* **22**, 66–79.

Ohta, T., Iijima, K., Miyamoto, M., Nakahara, I., Tanaka, H., Ohtsuji, M., Suzuki, T., Kobayashi, A., Yokota, J., Sakiyama, T., *et al.* (2008). Loss of Keap1 function activates Nrf2 and provides advantages for lung cancer cell growth. *Cancer Res.* **68**, 1303–1309.

Okawa, H., Motohashi, H., Kobayashi, A., Aburatani, H., Kensler, T. W., and Yamamoto, M. (2006). Hepatocyte-specific deletion of the keap1 gene activates Nrf2 and confers potent resistance against acute drug toxicity. *Biochem. Biophys. Res. Commun.* **339**, 79–88.

Padmanabhan, B., Tong, K. I., Ohta, T., Nakamura, Y., Scharlock, M., Ohtsuji, M., Kang, M. I., Kobayashi, A., Yokoyama, S., and Yamamoto, M. (2006). Structural basis for defects of Keap1 activity provoked by its point mutations in lung cancer. *Mol. Cell.* **21**, 689–700.

Priestley, J. R., Kautenburg, K. E., Casati, M. C., Endres, B. T., Geurts, A. M., and Lombard, J. H. (2015). The Nrf2 knockout rat: a new animal model to study ndothelial dysfunction, oxidant stress, and microvascular rarefaction. *Am. J. Physiol. Heart Circ. Physiol.* **310**, H478-87 ajpheart 00586 02015.

Roebuck, B. D., Johnson, D. N., Sutter, C. H., Egner, P. A., Scholl, P. F., Friesen, M. D., Baumgartner, K. J., Ware, N. M., Bodreddigari, S., Groopman, J. D., *et al.* (2009). Transgenic expression of aflatoxin aldehyde reductase (AKR7A1) modulates aflatoxin B-1 metabolism but not hepatic carcinogenesis in the rat. *Toxicol. Sci.* **109**, 41–49.

Scholl, P. F., McCoy, L., Kensler, T. W., and Groopman, J. D. (2006). Quantitative analysis and chronic dosimetry of the aflatoxin B1 plasma albumin adduct Lys-AFB1 in rats by isotope dilution mass spectrometry. *Chem. Res. Toxicol.* **19**, 44–49.

Singh, A., Misra, V., Thimmulappa, R. K., Lee, H., Ames, S., Hoque, M. O., Herman, J. G., Baylin, S. B., Sidransky, D., Gabrielson, E., *et al.* (2006). Dysfunctional KEAP1-NRF2 interaction in non-small-cell lung cancer. *PLoS Med.* **3**, e420.

Skoko, J. J., Wakabayashi, N., Noda, K., Kimura, S., Tobita, K., Shigemura, N., Tsujita, T., Yamamoto, M., and Kensler, T. W. (2014). Loss of Nrf2 in mice evokes a congenital intrahepatic shunt that alters hepatic oxygen and protein expression gradients and toxicity. *Toxicol. Sci.* **141**, 112–119.

Solt, D. B., Medline, A., and Farber, E. (1977). Rapid emergence of carcinogen-induced hyperplastic lesions in a new model for the sequential analysis of liver carcinogenesis. *Am. J. Pathol.* **88**, 595–618.

Suh, J. H., Shenvi, S. V., Dixon, B. M., Liu, H., Jaiswal, A. K., Liu, R. M., and Hagen, T. M. (2004). Decline in transcriptional activity of Nrf2 causes age-related loss of glutathione synthesis, which is reversible with lipoic acid. *Proc. Natl. Acad. Sci. USA.* **101**, 3381–3386.

Suzuki, T., Shibata, T., Takaya, K., Shiraishi, K., Kohno, T., Kuitoh, H., Tsuta, K., Furuta, K., Goto, K., Hosoda, F., *et al.* (2013). Regulatory nexus of synthesis and degradation deciphers cellular Nrf2 expression levels. *Mol. Cell. Biol.* **33**, 2402–2412.

Taguchi, K., Hirano, I., Itoh, T., Tanaka, M., Miyajima, A., Suzuki, A., Motohashi, H., and Yamamoto, M. (2014). Nrf2 enhances cholangiocyte expansion in Pten-deficient livers. *Mol. Cell. Biol.* **34**, 900–913.

Taguchi, K., Maher, J. M., Suzuki, T., Kawatani, Y., Motohashi, H., and Yamamoto, M. (2010). Genetic analysis of cytoprotective functions supported by graded expression of Keap1. *Mol. Cell. Biol.* **30**, 3016–3026.

Taguchi, K., Motohashi, H., and Yamamoto, M. (2011). Molecular mechanisms of the Keap1-Nrf2 pathway in stress response and cancer evolution. *Genes Cells* **16**, 123–140.

Taguchi, K., and Yamamoto, M. (2015). Keap1-Nrf2 regulatory system and cancer, Chapter 17. In Inoue J and Takekawa M. *Protein modifications in pathogenic dysregulation of signaling*. Springer Japan, 269-285.

Wakabayashi, N., Itoh, K., Wakabayashi, J., Motohashi, H., Noda, S., Takahashi, S., Imakado, S., Kotsuji, T., Otsuka, F., Roop, D. R., *et al.* (2003). Keap1-null mutation leads to postnatal lethality due to constitutive Nrf2 activation. *Nat. Genet.* **35**, 238–245.

Wang, X. J., Sun, Z., Villeneuve, N. F., Zhang, S., Zhao, F., Li, Y., Chen, W., Yi, X., Zheng, W., Wondrak, G. T., *et al.* (2008). Nrf2 enhances resistance of cancer cells to chemo therapeutic drugs, the dark side of Nrf2. *Carcinogenesis* **29**, 1235–1243.

Watai, Y., Kobayashi, A., Nagase, H., Mizukami, M., McEvoy, J., Singer, J. D., Itoh, K., and Yamamoto, M. (2007). Subcellular localization and cytoplasmic complex status of endogenous Keap1. *Genes Cells* **12**, 1163–1178.

Wild, C. P., Hasegawa, R., Barraud, L., Chutimataewin, S., Chapot, B., Ito, N., and Montesano, R. (1996). Aflatoxin albumin adducts: a basis for comparative carcinogenesis between animals and humans. *Cancer Epidemiol. Biomarkers Prev.* **5**, 179-189.

Wild, C. P., and Turner, P. C. (2002). The toxicology of aflatoxins as a basis for public health decisions. *Mutagenesis* **17**, 471–481.

Yamada, J., Serikawa, T., Ishiko, J., Inui, T., Takada, H., Kawai, Y., and Okaniwa, A. (1985). Rats with congenital tremor and curled whiskers and hair. *Jikken Dobutsu* **34**, 183–188.

Yamashita, Y., Ueyama, T., Nishi, T., Yamamoto, Y., Kawakoshi, A., Sunami, S., Iguchi, M., Tamai, H., Ueda, K., Ito, T., *et al.* (2014). Nrf2-inducing anti-oxidation stress response in the rat liver–new beneficial effect of lansoprazole. *PLoS One* **9**, e97419.

Yamori, Y., Horie, R., Handa, H., Sato, M., and Fukase, M. (1976). Pathogenetic similarity of strokes in stroke-prone spontaneously hypertensive rats and humans. *Stroke* **7**, 46–53.

Yanagawa, T., Itoh, K., Uwayama, J., Shibata, Y., Yamaguchi, A., Sano, T., Ishii, T., Yoshida, H., and Yamamoto, M. (2004). Nrf2 deficiency causes tooth decolourization due to iron transport disorder in enamel organ. *Genes Cells* **9**, 641–651.

Yates, M. S., Kwak, M. K., Egner, P. A., Groopman, J. D., Bodreddigari, S., Sutter, T. R., Baumgartner, K. J., Roebuck, B. D., Liby, K. T., Yore, M. M., *et al.* (2006). Potent protection against aflatoxin-induced tumorigenesis through induction of Nrf2-regulated pathways by the triterpenoid 1-[2-cyano-3-,12-dioxooleana-1,9(11)-dien-28-oyl]imidazole. *Cancer Res.* **66**, 2488–2494.

Yeligar, S. M., Machida, K., and Kalra, V. K. (2010). Ethanol-induced HO-1 and NQO1 are differentially regulated by

HIF-1alpha and Nrf2 to attenuate inflammatory cytokine expression. *J. Biol. Chem.* **285**, 35359–35373.

Zavattari, P., Perra, A., Menegon, S., Kowalik, M. A., Petrelli, A., Angioni, M. M., Follenzi, A., Quagliata, L., Ledda-Columbano, G. M., Terracciano, L., *et al.* (2015). Nrf2, but not beta-catenin, mutation represents an early event in rat hepatocarcinogenesis. *Hepatology* **62**, 851–862.

Zhang, P., Singh, A., Yegnasubramanian, S., Esopi, D., Kombairaju, P., Bodas, M., Wu, H., Bova, S. G., and Biswal, S. (2010). Loss of Kelch-like ECH-associated protein 1 function in prostate cancer cells causes chemoresistance and radioresistance and promotes tumor growth. *Mol. Cancer Ther.* **9**, 336–346.

Zhang, Y. K., Wu, K. C., and Klaassen, C. D. (2013). Genetic activation of Nrf2 protects against fasting-induced oxidative stress in livers of mice. *PLoS One* **8**, e59122.

Zhu, X., Xu, Y., Yu, S., Lu, L., Ding, M., Cheng, J., Song, G., Gao, X., Yao, L., Fan, D., *et al.* (2014). An efficient genotyping method for genome-modified animals and human cells generated with CRISPR/Cas9 system. *Sci. Rep.* **4**, 6420.